MIT-GFR-003

Aerodynamic Design of Turbine for S-CO_2 Brayton Cycle

Yong Wang

June 2003

Center for Advanced Nuclear Energy Systems
Department of Nuclear Engineering
Massachusetts Institute of Technology
Cambridge, MA 02139-4307

This work was supported by Idaho National Engineering and Environment Laboratory under the Strategic INEEL/MIT Nuclear Research Collaboration for Sustainable Nuclear Energy.

Introduction

The supercritical CO_2 (S-CO_2) Brayton cycle is proposed for Generation IV reactor applications because of its simplicity, high efficiency, compactness and thus potential to cost reduction. To achieve an attractive cycle efficiency (~ 45%), highly efficient cycle components must be guaranteed. Hence the turbine, the main design objective is to achieve high efficiency while maintaining the turbine at a reasonable size. Due to the high power and high mass flow rate demands of the present application an axial-flow turbine was employed. Two NASA Glenn Research Center (GRC) developed codes (TURBAN and AXOD) were modified and implemented to perform the aerodynamic design. TURBAN is a preliminary axial-flow turbine design code. AXOD is a multi-stage turbine off-design performance code. Both codes were developed for air-breathing aircraft engine and ideal gas applications. Since CO_2 exhibits significantly non-ideal behavior under S-CO_2 cycle operating conditions, both codes were modified to apply for real gas applications. The NIST pure fluid properties database was implemented into the codes for this purpose. TURBAN-MOD and AXOD-MOD are the modified versions respectively. TURBAN-MOD determines the stage velocity diagrams, stage and overall efficiencies and simple blade geometry at a design-point. AXOD-MOD calculates the off-design performance at optimum incidence angles based on the design-point and generates characteristic maps. The off-design performance maps can be used for cycle control analysis.

CO_2 Turbine Design

Design Conditions

Design conditions for a representative supercritical CO_2 Brayton cycle turbine are shown in Table 1, as proposed by Dostal[1].

Table 1. Design conditions for S-CO_2 turbine

Working fluid	Inlet total pressure (MPa)	Inlet total temperature(^oC)	Mass flow rate (kg/s)	Turbine power (MW)	Rotation speed (RPM)
CO_2	19.4	550	3644	450	3600

Using carbon dioxide (CO_2) as a working fluid has two major advantages over the conventional working fluid, Helium (He) for nuclear reactors: Firstly more net work can be extracted from the cycle due to the reduction in compression work when the compressor works in the vicinity of the critical point; and secondly a compact turbine can be achieved due to the high density of CO_2, which implies cost saving and simplicity of mechanical design.

A high turbine inlet total pressure is required in the S-CO_2 Brayton cycle. The benefit of high pressure is evident: higher pressures make CO_2 denser, which decreases the throughflow area and results in smaller volumetric flow rate when axial velocity is unchanged. The resulting overall turbine size will be reduced significantly. However, the high pressure also imposes some problems. For example, this high pressure complicates the turbine case design. Pressure loss is another issue of concern. Leakage at tip clearances and also inter-stage can be very significant under the high-pressure differential conditions, which will reduce the efficiency of the turbine. Therefore, seal design will be a major challenge for future work.

The moderate turbine inlet total temperature will not require cooling of the turbine blades, which greatly decreases the complexity of the blade detailed design and manufacturing. It also provides a relatively favorable environment under which the turbine operates, thus increasing the turbine life. In addition, the moderate temperature imposes less of a challenge to structural materials, allowing for a broader selection of materials for the turbine.

Figure 1 overviews operating regimes of different kinds of turbines. The aircraft gas turbine, due to its different application, runs at a higher temperature and lower pressure compared to power cycle turbines. The S-CO_2 cycle gas turbine, compared to its

major competitor helium cycle turbine, has a higher inlet pressure and moderate temperature. The benefit of such operating conditions has been indicated earlier.

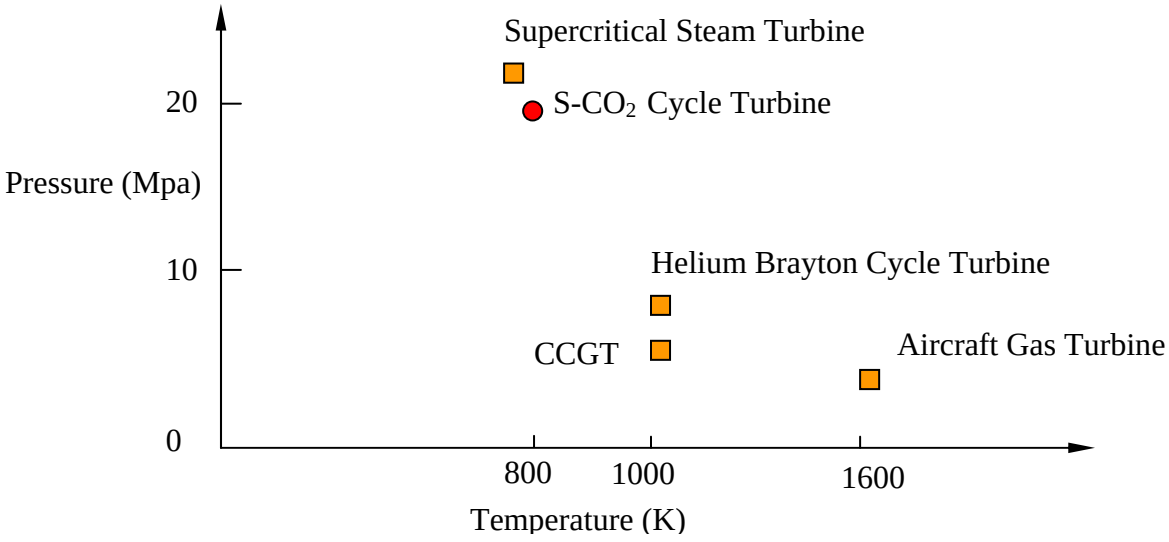

Figure 1. Operating conditions for power cycle turbines and aircraft gas turbine

TURBAN Descriptions

The preliminary turbine design was performed based on a NASA-developed code (TURBAN). TURBAN is a mean-line analysis code, which doesn't include radial gradients of the flow properties in the flow and efficiency calculations. The code as written is only applicable for ideal gas assumptions. Since CO_2 exhibits significantly non-ideal behavior over the range of S-CO_2 cycle operating conditions of interest, the original code was modified to apply for real gas applications. The code modifications and validation will be discussed in the following section.

The required inputs include shaft power POW, mass flow rate W, inlet total pressure Pt_{in}, inlet total temperature Tt_{in}, rotational speed N, inlet mean diameter D_{in}, exit mean diameter D_{ex}, nozzle exit angle α_1, gas constant Rg. The number of stages n and the type of velocity diagrams are also specified.

The first and last stage blade speeds are calculated based on the input mean diameters and rotational speed. For more than two stages, linear variation is assumed to obtain the blade speeds of the other stages.

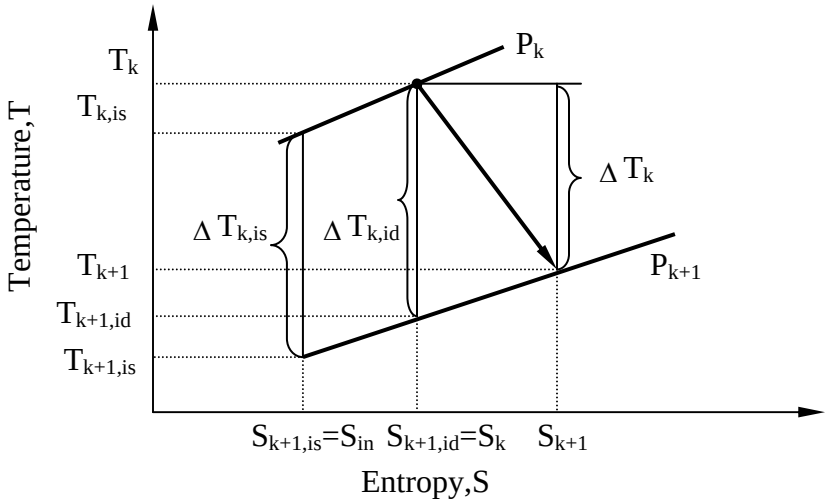

Note: Values in the figure are total state quantities and Cp is a constant.

Figure 2. Temperature- entropy diagram for k^{th} stage

Referring to Figure 2, turbine overall total efficiency is defined as:

$$\eta_t = \frac{\sum Cp \cdot \Delta T_k}{\sum \left(\frac{T_{k,is}}{T_k} \right) \cdot Cp \cdot \Delta T_{k,id}} \qquad (1)$$

Where η_t is total-to-total efficiency, Cp is specific heat capacity, ΔT_k and $\Delta T_{k,id}$ are actual and ideal temperature drops across a stage respectively, T_k is stage inlet temperature and $T_{k,is}$ is stage isentropic inlet temperature which is defined so that expansion from turbine inlet to a stage inlet is isentropic.

Equation (1) can be also rewritten into

$$\eta_t = \frac{1}{\sum \left(\frac{T_{k,is}}{T_k} \right) \cdot \left(\frac{1}{\eta_k} \right) \cdot \left(\frac{U_k^{\,2}}{\sum U_k^{\,2}} \right)} \qquad (2)$$

Where η_k is stage total efficiency and U_k is blade speed. The reheat effect is also accounted for in the above equation.

The stage efficiency computation method is fully explained by Steward[2] and only the key equations are presented in this section. Stage total efficiency can be expressed as:

$$\eta_k = \frac{1}{1 + \frac{A}{2} \cdot \lambda} \tag{3}$$

Where the working factor λ is defined as:

$$\lambda = \frac{\sum \Delta H_k}{\sum U_k^{\,2}} \tag{4}$$

While the stage loss parameter A is

$$A = \frac{K \cdot \mathrm{Re}^{-0.2}}{\cot \alpha_1} \cdot \left(F_{st} C_{st} + F_{ro} C_{ro} + C_{ev} \right) \tag{5}$$

A loss coefficient value K of 0.3[3] is recommended for use in the absence of additional information. This value was calibrated on several different design systems that cover a wide range of design characteristics. However, a conservative value of 0.4 was used in our turbine design and analysis due to its high-pressure application. The Reynolds number used in this calculation is defined as:

$$\mathrm{Re} = \frac{2w}{\mu \cdot D_{in}} \tag{6}$$

The rotor-weighting factor F_{ro} and rotor loss parameter C_{ro} are the same for all cases:

$$F_{ro} = 2 \tag{7}$$

$$C_{ro} = 2\cot^2\alpha_1\left(\frac{V_{u,1}}{\Delta V_u}\right)^2 + \left(\frac{V_{u,1}}{\Delta V_u} - \lambda\right)^2 + \left(\frac{V_{u,2}}{\Delta V_u} - \lambda\right)^2 \qquad (8)$$

The relations between $V_{u,1}$, $V_{u,2}$ and ΔV_u are displayed in Figure 3, which also apply for the following equations. V_1 and V_2 are absolute velocities at station 1 and 2 respectively (or rotor inlet and exit). W_1 and W_2 are relative velocities. $V_{x,1}$ and $V_{x,2}$ are axial velocities. $V_{u,1}$ and $V_{u,2}$ are tangential component of absolute velocities and ΔV_u is tangential velocity difference.

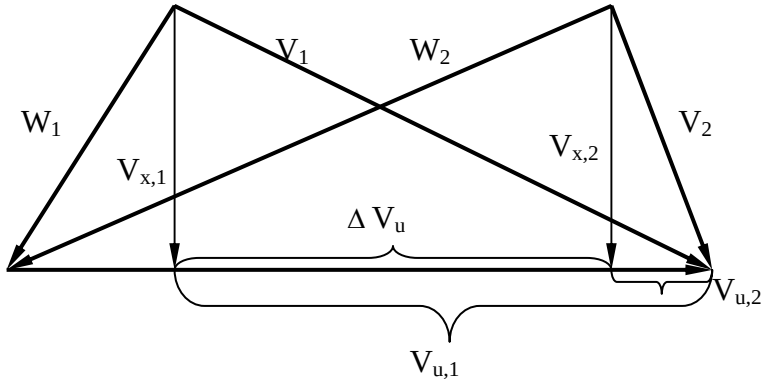

Figure 3. Typical turbine velocity diagram

For last stages of turbines having exit vanes, the exit vane loss parameter is expressed as:

$$C_{ev} = 2\cot^2\alpha_1\left(\frac{V_{u,1}}{\Delta V_u}\right)^2 + \left(\frac{V_{u,2}}{\Delta V_u}\right)^2 \qquad (9)$$

For all other stages

$$C_{ev} = 0 \qquad (10)$$

For first-stage stators having a specified inlet angle α_0, the stator loss parameter is expressed as:

$$C_{st} = \left[1 + \cot^2\alpha_1\left(2 + \tan^2\alpha_0\right)\right]\left(\frac{V_{u,1}}{\Delta V_u}\right)^2 \qquad (11)$$

For all other stators

$$C_{st} = \left(1 + 2\cot^2 \alpha_1\right)\left(\frac{V_{u,1}}{\Delta V_u}\right)^2 + \left(\frac{V_{u,2}}{\Delta V_u}\right)^2 \tag{12}$$

The stator-weighting factor also depends on whether or not the stator is a first-stage stator. For a first stage stator having a specified inlet angle α_0,

$$F_{st} = \frac{1 - \dfrac{3\tan\alpha_0}{\tan\alpha_1}}{1 - \dfrac{\tan\alpha_0}{\tan\alpha_1}} \tag{13}$$

For all other stators

$$F_{st} = \frac{1 - \dfrac{3\left(V_{u,2} \big/ \Delta V_u\right)}{\left(V_{u,1} \big/ \Delta V\right)}}{1 - \dfrac{\left(V_{u,2} \big/ \Delta V_u\right)}{\left(V_{u,1} \big/ \Delta V\right)}} \tag{14}$$

In order to determine the number of blades and blade chord length, a cascade loading model to compute axial solidity (ratio of blade chord axial projection to blade spacing) and a blade geometry model to compute stagger angle are used in the code[4]. Axial solidity, as derived by Zweifel[5] depends on the blade inlet and exit flow angles and on the tangential loading coefficient (the ratio of actual blade loading to Zweifel's ideal loading). The blade stagger angle calculation is based on a blade geometry having a suction surface with circular-arc turning and straight transition sections at inlet and exit.

Code Modifications (TURBAN-MOD)

As mentioned above, TURBAN itself was originally used to perform our CO_2 turbine design and analysis but is applicable only for ideal gas assumptions. Unfortunately CO_2 exhibits significant non-ideal behavior over the range of operating conditions of interest. It was observed that the ideal gas treatment for CO_2 under the operating conditions of our turbine gives about 10.8 percent higher power than the real gas case, see Table 2. This discrepancy was resolved by replacing correlations derived under ideal gas assumptions with real gas properties. The NIST pure fluid property database[6] was used to provide real fluid properties via interpolation.

Table 2. Comparison of real gas and ideal gas treatments

Power Target: 450MW

Input

	Ideal Gas	Real Gas
Mass Flow Rate (kg/s)	3644	3644
Inlet Total Temperature (K)	823	823
Inlet Total Pressure (MPa)	19.4	19.4
Inlet Total Enthalpy (kJ/kg)	N/A	1035.78

Output

	Ideal Gas#	Real Gas*
Exit Total Temperature (K)	709.883	711.356
Exit Total Pressure (MPa)	7.608	7.713
Exit Total Enthalpy (kJ/kg)		897.996
Total Enthalpy Difference (kJ/kg)	$(Cp.\Delta T)$ 136.87	$(H_{in}-H_{ex})$ 123.515
Power (MW)	498.8	450.1
Error (%)	10.8	0.02

Cp = 1.21 for calculations in ideal case.
* Real gas calculations were performed after code modifications were complete.

For an ideal gas with known inlet conditions and stage efficiency, the exit pressure is readily determined using the isentropic relation:

$$P_{t,k+1} = P_{t,k}\left(\frac{T_{t,k+1,id}}{T_{t,k}}\right)^{\gamma/\gamma-1} \tag{15}$$

Where $P_{t,k}$ and $T_{t,k}$ are stage inlet stagnation pressure and temperature. $P_{t,k+1}$ is exit pressure and $T_{t,k+1,id}$ is ideal exit temperature which is defined such that the expansion process from stage inlet pressure to stage exit pressure is isentropic. γ is specific heat ratio.

This relation does not hold for a real gas. In order to calculate the exit total pressure, inlet total entropy and total enthalpy are obtained by interpolation based on inlet total temperature and pressure. Ideal exit total enthalpy (flow expands from inlet to exit isentropically) is then computed in terms of the stage work and stage efficiency. From the entropy and ideal exit total enthalpy, the exit total pressure is then calculated. Once the exit enthalpy and pressure are known, the other properties can be easily derived. The calculation procedure is more evidently shown in Figure 4.

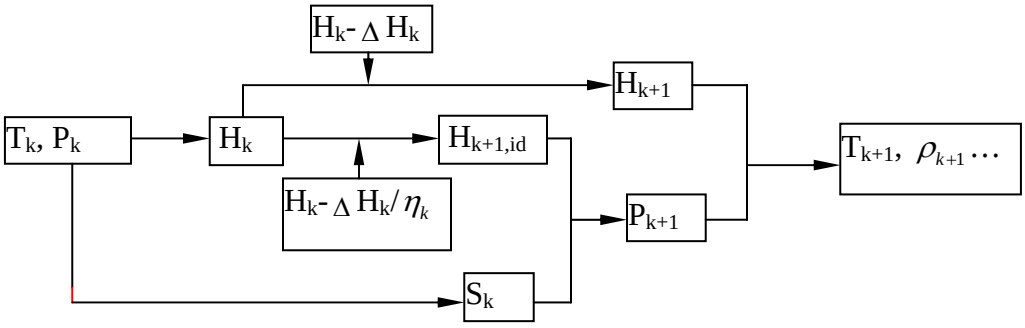

Figure 4. Calculation procedure for k[th] stage

The relations between the stagnation and static conditions are also dealt with in a similar manner. Instead of using the relations

$$\begin{cases} P_s = P_t\left(1+\dfrac{\gamma-1}{2}M^2\right)^{\frac{-\gamma}{\gamma-1}} \\ T_s = T_t\left(1+\dfrac{\gamma-1}{2}M^2\right)^{-1} \end{cases} \tag{16}$$

(Where subscript “s” denotes static state condition and “t” total state condition and M is Mach number defined as the ratio of local velocity to local speed of sound), one derives the static conditions based on the fact that the thermodynamic process of moving between the static and stagnation states is isentropic. The stagnation (total) entropy and stagnation enthalpy are first calculated on the basis of total state conditions. Then static enthalpy is obtained by Equation (17)

$$H_s = H_t - V^2 \big/ 2 \tag{17}$$

Since the total entropy is identically equal to the static entropy, other static properties can then be determined from the property database via interpolation based upon entropy and static enthalpy.

The first term of the denominator in Equation (2) which represents the reheat effect is no longer valid for real gas since it assumes specific heat capacity at constant pressure Cp is unchanged across the turbine. Therefore, enthalpy H is used in lieu of temperature to calculate the reheat effect and equation (2) is accordingly rewritten as:

$$\eta_t = \frac{1}{\sum \left(\frac{H_{k,is}}{H_k} \right) \cdot \left(\frac{1}{\eta_k} \right) \cdot \left(\frac{U_k^{\,2}}{\sum U_k^{\,2}} \right)} \tag{18}$$

With increase in entropy, the enthalpy difference between two iso-bar lines will increase accordingly. That is, ideal enthalpy difference across a stage $\Delta H_{k,id}$ is greater than ideal enthalpy difference $\Delta H_{k,is}$ which is based on turbine inlet, as shown in Figure 5. To account for this variation, Equation (19) is applied to derive the isentropic enthalpy.

$$\begin{cases} \Delta H_{k,is} = \dfrac{\Delta H_k}{\eta_k} \dfrac{H_{k,is}}{H_k} \\ H_{k+1,is} = H_{k,is} - \Delta H_{k,is} \end{cases} \tag{19}$$

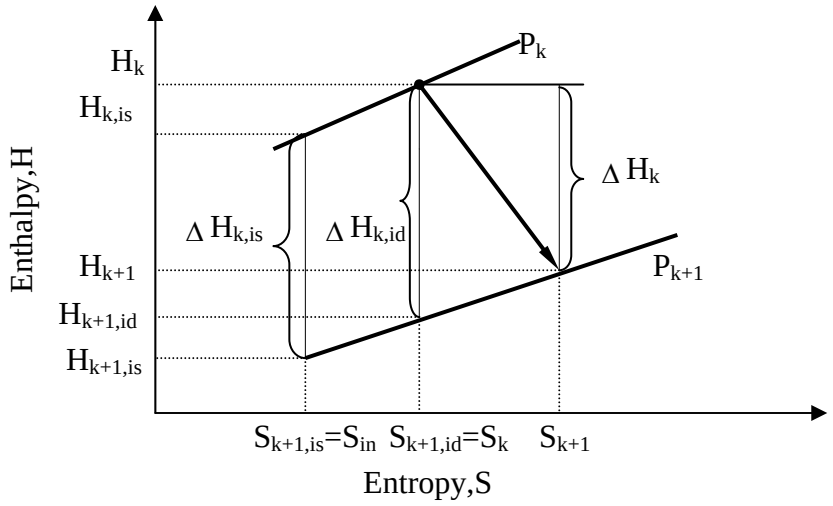

Note: Values in the figure are total state quantities.

Figure 5. Enthalpy-entropy diagram for k^{th} stage

Two approaches were performed and compared to prove the validity of the modified reheat effect in terms of flow condition calculations for each stage. The first way considers the isentropic expansion from the turbine inlet to the exit of the stage of interest. The alternative way follows the isentropic expansion across an individual stage of interest, that is, based on the stage inlet entropy and stage ideal exit enthalpy one computes pressure by interpolation. The comparison between these two approaches is shown in Figure 6. In the first analysis (6a), stage exit enthalpy H_k is firstly computed based on the known upstream conditions (stage inlet) and stage efficiency. Then stage ideal enthalpy $H_{k,id}$ is calculated with consideration of the reheat effect. With known ideal enthalpy and turbine inlet entropy, pressure can be calculated by interpolation. Then based upon the pressure and actual enthalpy, other flow properties are readily determined by interpolation. In the latter approach (6b), the stage isentropic enthalpy $H_{k,is}$ is computed using stage inlet information and stage efficiency. An iso-pressure line is then determined by isentropic enthalpy and stage inlet entropy. On the basis of this resultant pressure and actual enthalpy, other information at the stage exit is determined. Comparison shows that the flow conditions from these two approaches are in good agreement, which implies that the modified reheat effect is correct.

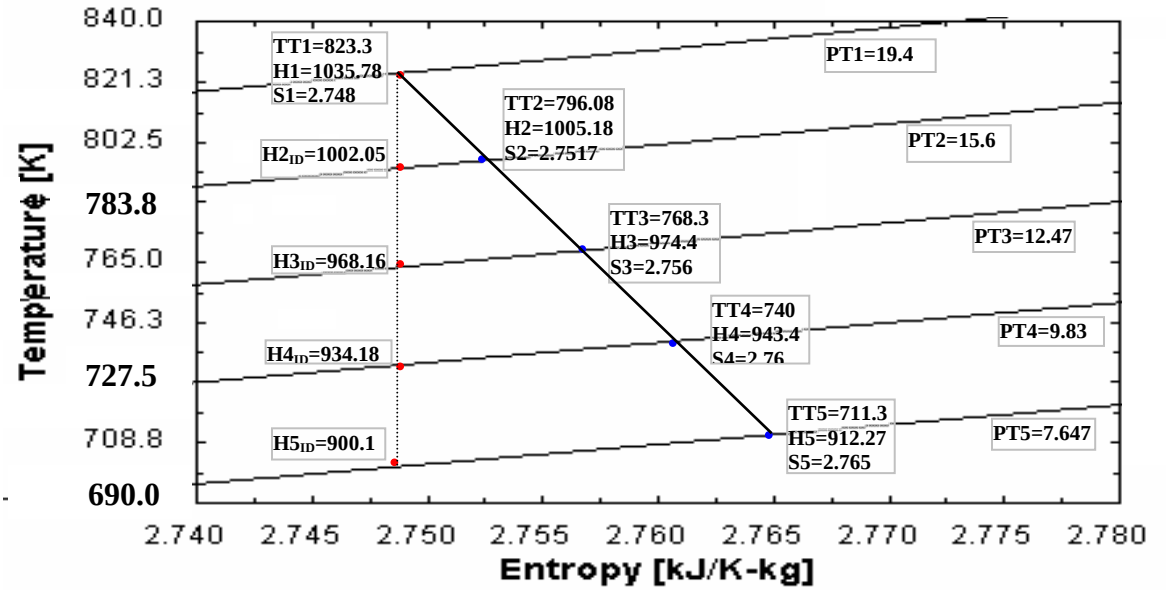

(6a): first approach

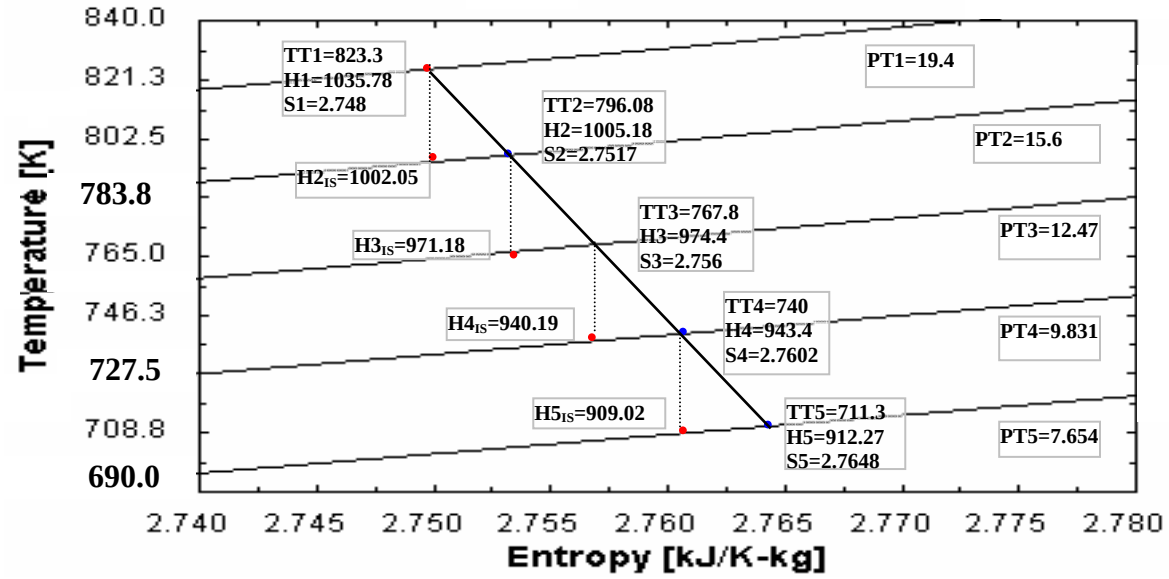

(6b): Second approach

Figure 6. Two approaches of reheat effect modification validation

Note: the units of enthalpy and total pressure in Fig. 6 are kJ/kg and MPa respectively.

Prior to utilizing the modified version of the code (TURBAN-MOD), helium was used to validate it since helium is considered to be an ideal gas within the operating range of interest. The input variables are referenced to the operating conditions in a Helium Brayton cycle with one compressor established by Dostal[1]. That is, turbine inlet temperature is 1153K, inlet pressure is 8 MPa, mass flow rate is 472.21 kg/s and turbine output power is 550.05 MW. Then Helium was treated as an ideal gas in TURBAN and as a real gas in TURBAN-MOD respectively. The major results including turbine inlet, exit tip and hub diameters, turbine total-to-static adiabatic efficiency based on the optimum values (120 in inlet and exit mean diameters and 68^o of stator exit angle) are compared in Table 3. The results are in perfect agreement, which indicates that the coding modifications in TURBAN-MOD are valid.

Table 3. Helium turbine results from TURBAN and TURBAN-MOD

		TURBAN (ideal)	TURBAN-MOD (real)
Efficiency (%)	Total	92.5	92.5
	Static	90.8	90.8
Inlet Diameters (m)	Tip	3.122168	3.12293
	Hub	2.973832	2.97307
Exit Diameters (m)	Tip	3.14706	3.147568
	Hub	2.94894	2.948432

Parametric Study and Results

Once the modifications were complete, the code was ready for turbine design analysis. In the general case, TURBAN-MOD is applicable for any working fluid as long as fluid properties are called from NIST subroutines.

The design objective is to optimize the adiabatic efficiency of the turbine while maintaining the turbine at a reasonable size. Since the flow exiting from the turbine will not be recovered in the recuperator, only the static efficiency, which is defined as the ratio of total enthalpy difference across the turbine to the enthalpy difference between the inlet total and exit ideal static enthalpy, will be considered in the following discussion. The static efficiency is usually lower than the total efficiency since it considers the exit kinetic energy as a loss. Design variables studied herein are number of stages, inlet and

exit mean diameters, stator exit angle and degree of reaction. The optimization of design variables is analyzed in the following sections.

Effect of number of stages

As shown in Figure 7(a), total-to-static (static hereafter) efficiency increases with the number of stages. The number of stages affects static efficiency only slightly when it exceeds a value of 4. However, turbine exit tip and hub diameters which represent the turbine size show an almost linear increase with the number of stages as indicated in Figure 7(b). This is because when the number of the stages increases, the work loading of each stage decreases when constant mean diameters hold, resulting in a decrease in axial flow velocity. The reduced axial velocity requires greater annulus area for a certain mass flow. Since another design objective is to reduce the turbine size (from a cost prospective), and the efficiency difference between four stages and more is negligible, the four-stage design is therefore inferred to be optimal.

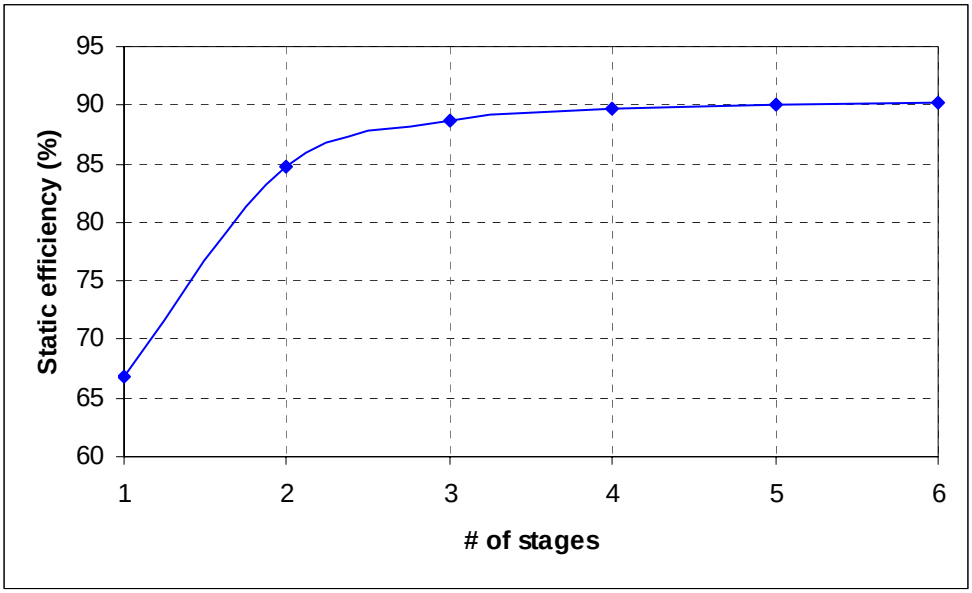

(a) Efficiency vs. number of stages

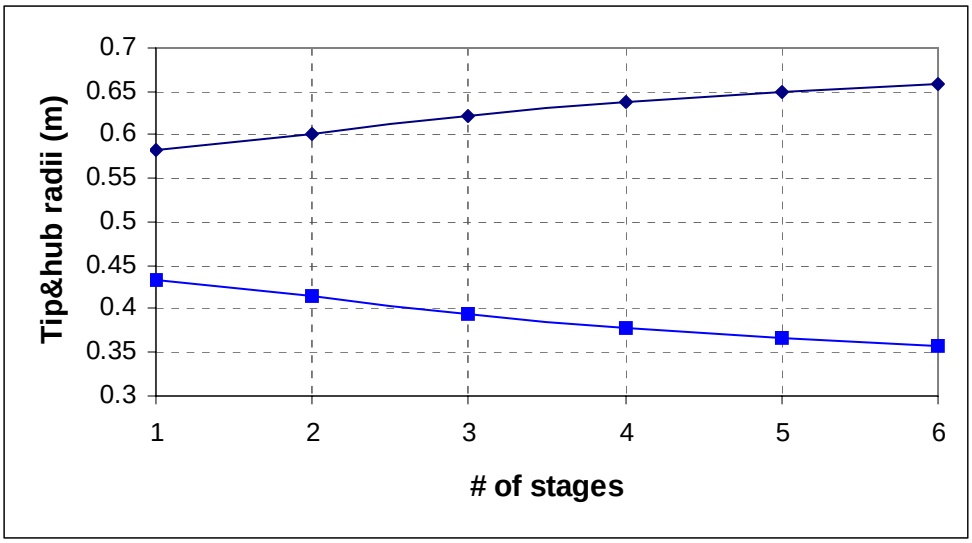

(b) Turbine radii vs. number of stages

Figure 7*. Effect of number of stages

*Fixed parameters used in the stage number optimum analysis are: inlet and exit mean diameter $Dm_{in}=Dm_{ex}=1.016$ m, stator exit angle $\alpha_1=66^o$, degree of reaction =0.5.

Effect of vane exit angle

Figure 8 shows that the static efficiency first increases with the vane exit angle, and then drops. Increase in exit angle results in a decrease in the effective area for through-flow. In order to pass a certain amount of flow without choking, the annulus area will expand. The result is slowing the axial speed at the turbine exit. In addition, the total efficiency does not decrease significantly at first. Therefore, the static efficiency goes up. When exit angle exceeds a certain value, the total efficiency drops significantly, and large flow turning causes severe flow separation at the vane exit, which contributes a significant loss of turbine efficiency; the static efficiency decreases quickly. Thus, there is an optimum vane exit angle to achieve maximum efficiency. Figure 8 indicates 66^o is an optimum.

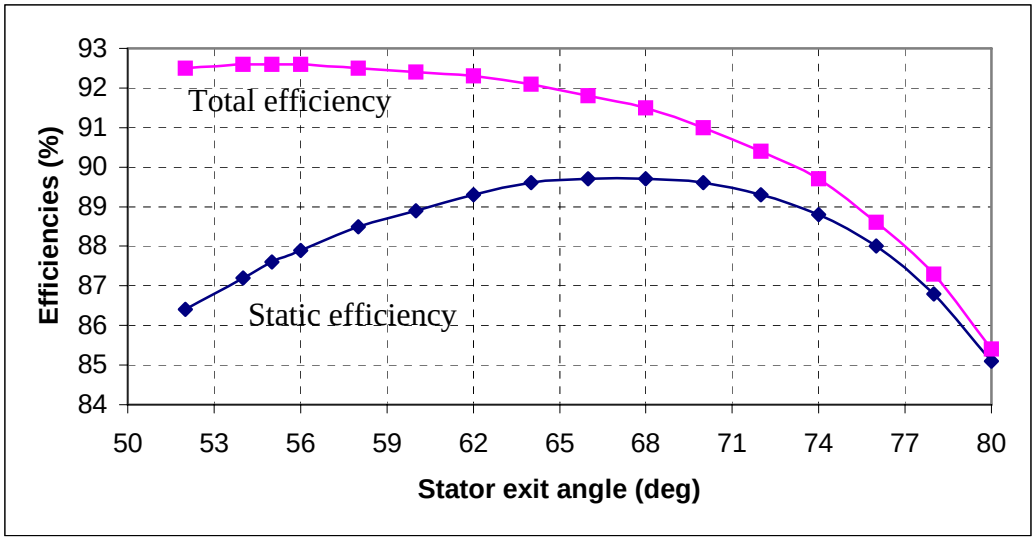

Fixed parameters: inlet and exit mean diameter = 1.016 m, number of stages = 4, degree of reaction = 0.5.

Figure 8. Efficiencies vs. vane exit angle

Effect of mean diameter

Constant mean diameters were firstly assumed for preliminary design. The effect of the mean diameters on the static efficiency is shown in Figure 9. At smaller mean diameters, the stage loading coefficients are rather larger than the desired value which Fielding[7] indicates as 1.0-1.5. The total efficiency is low and the corresponding static efficiency is low as well. At greater mean diameters, in contrast, the stage loading coefficients are much lower than the desired value. In addition, due to the decrease in annulus area, the gas leakage also contributes to the further decrease in static efficiency. Therefore, an optimum value exits and is about 1.02 m as indicated in Figure 9.

Effect of degree of reaction

In the general case, it is desired to have the degree of reaction in the vicinity of 0.5[8] to ensure the low friction loss. However, in high pressure turbine leakage loss may be significant. In order to decrease the leakage loss, low reaction blade should be adopted to keep the static pressure differential small across the rotor. This tradeoff must be studied before the value of degree of reaction is selected. Unfortunately the leakage loss

model is not available in our current design code. Therefore, a tentative value of 0.5 is used in this analysis. But further work on the effect of degree of reaciton should be conducted in the detailed design.

Based upon the above analysis, the optimum design variables are number of stages equal to 4, vane exit angle of 66^o, inlet and exit turbine mean blade diameter of 1.106 m and degree of reaction of 0.5.

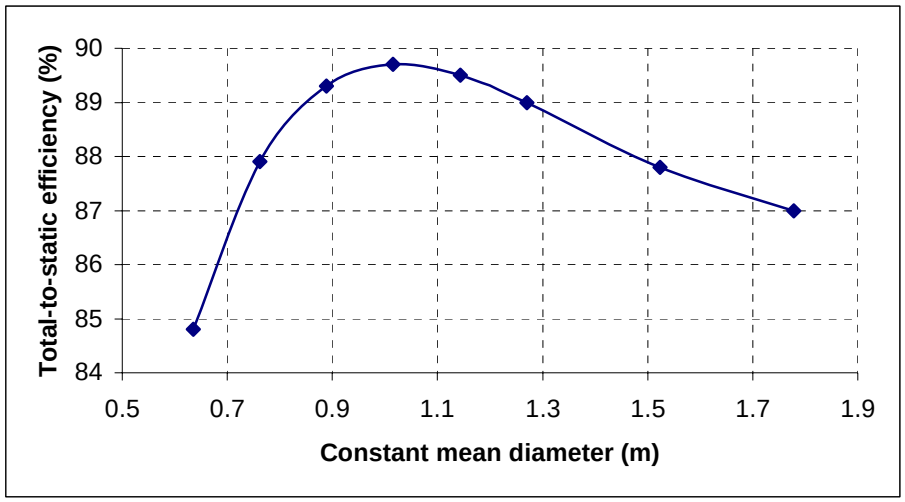

Fixed parameters: number of stages = 4, stator exit angle α_1 =66^o, degree of reaction =0.5.

Figure 9. Efficiency vs. blade mean diameter

The following analysis and resulting turbine preliminary size design were both based upon the optimum design variables and the imposed operating conditions. Once again, a conservative value of turbine loss coefficient K=0.4 is selected for our high-pressure application. Tables 4-6 show the corresponding outputs from TURBAN-MOD.

Table 4. Turbine mean section results

# of stages		4	Stg Work Factor		0.84	Reynolds #		2.071*10^8	Deg of React		0.5
Exit Tip Diam	[m]	1.275	Exit Total Temp	[K]	711.356	Stat. Exit Ang	[deg]	66	First Stg. Mn Spd	[m/s]	191.512
Exit Hub Diam	[m]	0.757	Exit Stat. Temp	[K]	708.411	Stg Exit. Ang	[deg]	10.93	Last Stg Mn Spd	[m/s]	191.512
Exit Rad Ratio		0.5941	Exit Tot. Press	[MPa]	7.713	Rotor Inl. Ang	[deg]	-10.93	Last Stg Inl Swirl	[m/s]	176.351
Inlet Tip Diam	[m]	1.161	Exit. Stat Press	[MPa]	7.648	Rotor Exit Ang	[deg]	-66	Last Stg Exit Swirl	[m/s]	15.161
Inlet Hub Diam	[m]	0.871	T-T Press Ratio		2.516	Tot Efficiency		0.918	Last Stg. Merid Vel	[m/s]	78.52
Inlet Hub/Tip Ratio		0.7498	T-S Press Ratio		2.576	Stat. Efficiency		0.897	Exit Merid Ma #		0.1924
Last Stg M1 Abs		0.4771	Last Stg M1 Rel		0.1976	Last Stg M2 Rel		0.473	Last Stg M2 Abs		0.196
Stg React		0.5	Stg Tot Eff-Unc		0.914	Tot Eff-Unc		0.918	Tot Eff-Rot Prim		0.918

Table 5. Free-vortex results

HUB	Last Stg M1 Abs		0.6211	Last Stg M1 Rel		0.3049	Last Stg M2 Rel		0.3628	Last Stg M2 Abs	0.2024
	Vane exit Ang	[deg]	71.64	Rotro Inl Ang	[deg]	50.09	Rotor Exit Ang	[deg]	-57.32	Stg.Exit Ang [deg]	14.52
TIP	Last Stg M1 Abs		0.3967	Last Stg M1 Rel		0.3127	Last Stg M2 Rel		0.602	Last Stg M2 Abs	0.1982
	Vane exit Ang	[deg]	60.81	Rotro Inl Ang	[deg]	-51.79	Rotor Exit Ang	[deg]	-71.01	Stg.Exit Ang [deg]	8.75

Table 6. Blading geometry

	vane					Rotor					Stress (A*N**2) [$in^2.rev^2/s^2$]
Stage	Axial Chord [m]	Axial Solid	Actual Solid	Stagger Ang [deg]	# of Vanes	Axial Chord [m]	Axial Solid	Actual Solid	Stagger Ang [deg]	# of Blades	0.1659*10**11
1	0.055	0.929	1.515	52.18	53	0.055	0.849	1.481	-55.03	49	
2	0.055	0.849	1.481	55.03	49	0.055	0.849	1.481	-55.03	49	
3	0.055	0.849	1.481	55.03	49	0.055	0.849	1.481	-55.03	49	
4	0.055	0.849	1.481	55.03	49	0.055	0.849	1.481	-55.03	49	

Table 4 shows the computation results satisfying the input requirements. The temperatures, pressures, velocities and angles are meanline values and the continuity and efficiency calculations are based on these values.

Table 5 displays the hub and tip free-vortex values of Mach number and angles for the last stage, where the radial variation are the largest. These flow parameters do not enter into the continuity and efficiency calculations, but are shown only to indicate the severity of the radial variation.

Table 6 summarizes the blading geometries. Given for each stage are the chords, solidities, stagger angles and blade count for the vane and the rotor. The centrifugal stress parameter in the last stage is also shown.

The velocity triangles extracted from the output results at mean section, tip and hub locations are shown in Figure 10. The velocity triangles are assumed to be the same for all the stages in the analysis.

Meanline Velocity Triangle: (R=0.5)*

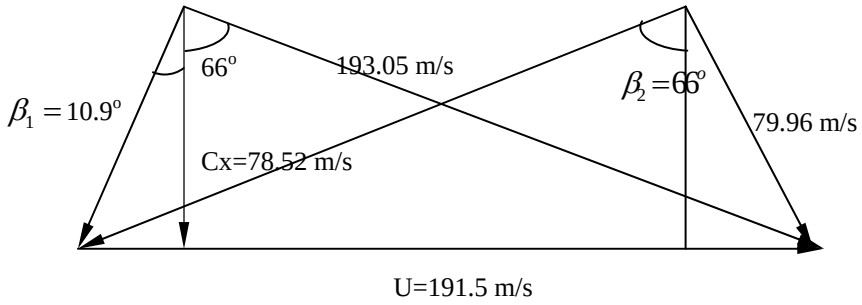

Tip Velocity Triangle: (R=0.694)*

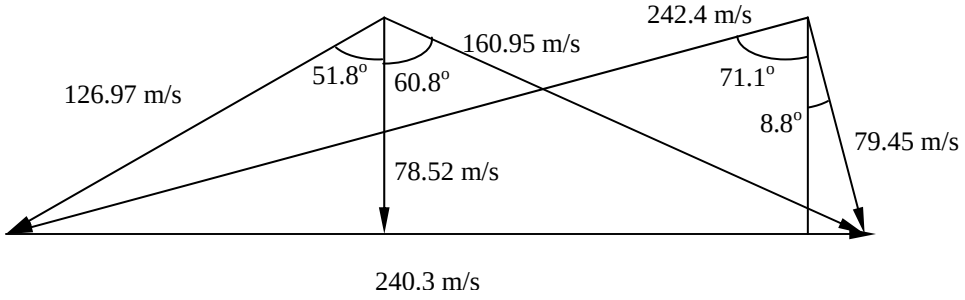

Hub Velocity Triangle: (R=0.101)*

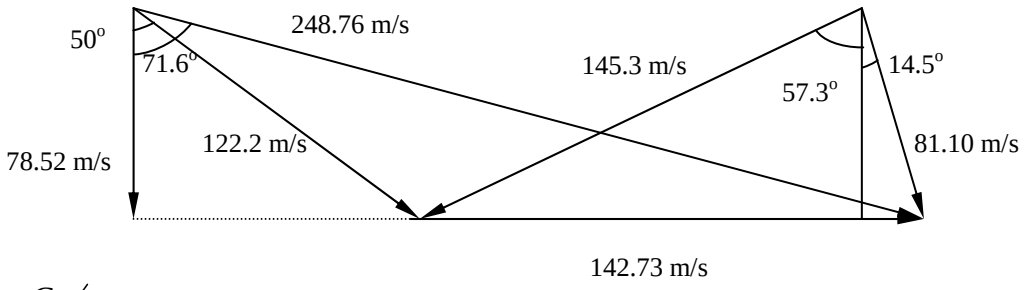

* $R = Cx/2U\left(\tan\beta_1 + \tan\beta_2\right)$

Figure 10. Velocity triangles at mean section, tip and hub

Sizes and shapes of turbine blade sections are also drawn schematically in Figure 11. As one can see, the maximum diameter is only about 51 inches (about 1.3m) and the entire length of the bladed section is about 0.6m, which is very compact and confirms the conclusion drawn by Dostal[1].

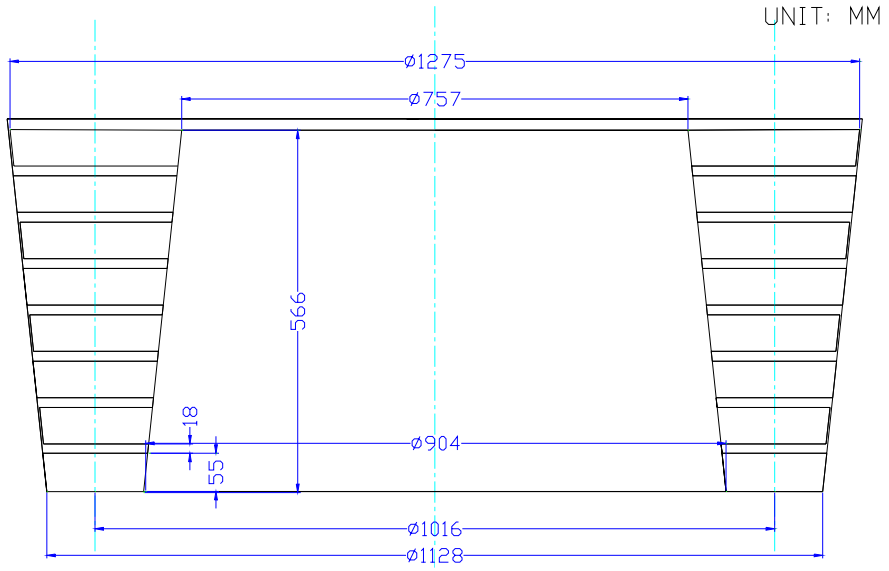

Figure 11. Schematic of turbine blade section

A S-CO_2 turbine designed by TURBAN-MOD is also compared with one designed by Muto[9] with the same operating conditions. As shown in Table 7, the results are in good agreement except for the numbers of nozzles and blades and efficiency. The difference in number of blades is probably attributable to the different aspect ratios and assumed blade thickness. The turbine designed by TURBAN-MOD used moderate aspect ratio. If higher aspect ratio is used, more blades will be needed. Muto's turbine also claims almost 1 percent higher efficiency than our turbine which is attributed to the fact that different loss models are used in the design analysis.

Table 7 Comparison of turbines designed by TURBAN-MOD and Muto

Input Condition:

Mass Flow Rate	Inlet Total Temperature	Inlet Total Pressure	Exit Total Pressure	Turbine Loss Coefficient	Mean Line Diameter
730 kg/s	800 deg C	7 MPa	1.712 MPa	0.3	1.178 m

Outputs Comparison			
Turbine		MUTO	TURBAN-MOD
Loading Coefficient		1.14	1.21
Flow Coefficient		0.419	0.418
Number of Stages		4	4
Hub Diameter [m]	Inlet	1.1	1.094
	Exit	1	0.967
Casing Diameter [m]	Inlet	1.25	1.262
	Exit	1.33	1.389
Number of Blades	Nozzle	263	176
	Rotor	421	248
Bladed Section Length [m]		0.81	0.625
Adiabatic Efficiency		93.40%	92.60%

MUTO

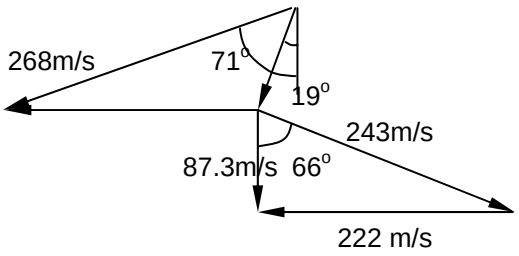

TURBAN-MOD

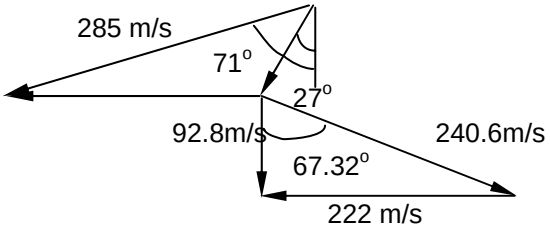

Off-design performance analysis

AXOD Description

Off-design analysis was performed using AXOD-MOD which is our in-house-modified version of AXOD. The original code, AXOD, was developd under the assumption of ideal gas applications. Up to 6 proportionally distributed area sectors can be specified, for each of which a quasi-one-dimensional calculation procedure is assumed. Total temperature, total pressure and axial velocity are also assumed constant across each sector. Static conditions and tangential component velocity vary as a free-vortex. The six radial area sectors are then joined utilizing simple radial equilibrium. The basic calculation for the equations of momentum, continuity and energy are performed at

the vane exit and the rotor exit stations. Definition of calculation stations is illustrated in Figure 12.

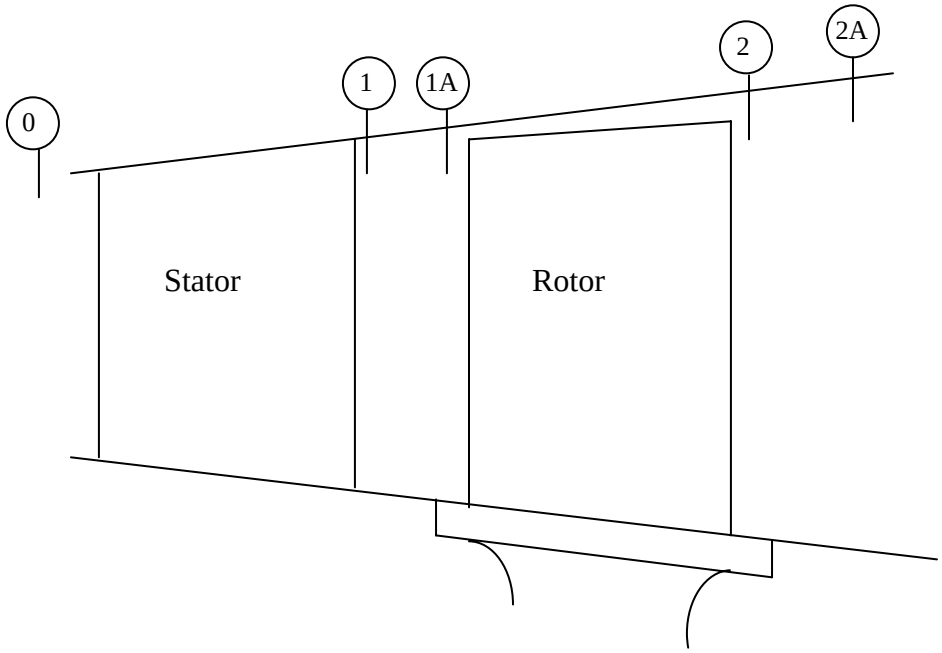

Figure 12. Definition of calculation stations

Three types of losses are considered for the off-design performance model: a blade-row inlet loss, a blade-row loss, and a stage test loss[10]. The blade-row inlet loss accounts for area-constriction and incidence effects at the inlet to each blade row by producing a reduction in blade-row inlet total pressure. Blade-row inlet loss is represented by a blade-row inlet kinetic energy recovery efficiency defined as:

$$\eta_{rec} = \eta_{rec,opt} \cos^{n}(I - I_{opt}) \qquad (20)$$

Where subscript "opt" denotes the optimum value. η_{rec} is recovery efficiency, I is incidence angle and n is the cosine-law exponent. Recommended exponent values are a positive-incidence exponent of 3 and a negative-incidence exponent of 4.

Blade-row loss is represented by a blade-row kinetic energy efficiency defined as:

$$\eta_b = \frac{actual \quad exit \quad kinetic \quad energy}{theoretical \quad exit \quad kinetic \quad energy} \tag{21}$$

For a stator, the stator efficiency is expressed in terms of absolute velocity:

$$\eta_s = \frac{V_1^2}{V_{1,id}^2} \tag{22}$$

Where V_1 is stator actual exit velocity and $V_{1,id}$ is ideal exit velocity without considering losses across the stator, i.e., the expansion process across the stator is isentropic. The relation between V_1 and $V_{1,id}$ is shown in Figure 13. Digital subscripts represent calculation station number.

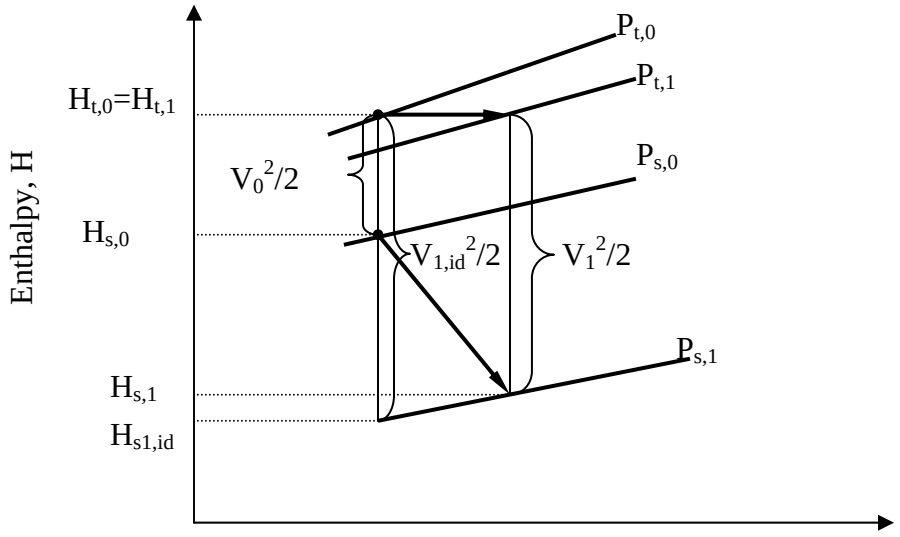

Figure 13. Expansion process across a stator

Rotor efficiency has a similar definition except that relative quantities with respect to a rotational frame are used instead of absolute values for the stator.

The stage test loss is represented by a stage test factor which is used to reflect losses that don't show up in the velocity diagrams. These can include clearance, disk friction, and mechanical losses.

The pure axial-flow assumption is not adequate for turbines with high flowpath slopes because of the presence of radial velocity. Treating the velocity component V_x as a meridional velocity and introducing a flow coefficient composed of a user-defined base value and a linear function of blade-row pressure ratio that reduces the flow coefficient by 2 percent going from low pressure ratio to choke, the continuity equation is rewritten as:

$$W = \sum C_{f,j} \rho_j A_{an,j} V_{x,j} \cos \varepsilon \qquad (23)$$

Where W is total mass flow through the annulus area, $C_{f,j}$ is the flow coefficient for each area sector, ε is the flowpath slope angle of each sector and $A_{an,j}$ is sector annulus area.

Because of a possible shift in sector pitch-line diameter due to the flowpath slope between the blade row exit and the following blade row inlet (for example, from station 1 to station 1A), the tangential component of velocity is adjusted inversely proportional to diameter to conserve the angular momentum. The axial component of velocity is adjusted for the annulus area change and density change between two neighboring blade rows.

Similarly, there may be a radial shift in pitch-line diameter as the working gas flows from the rotor inlet to the rotor exit station. In the relative coordinate system an additional work term appears due to the radial outflow or inflow. From the energy equation, the relative total enthalpy is adjusted proportional to the difference in wheel speed squared. There is no loss associated with radial flow shifts.

The input to the code mainly includes turbine inlet conditions, diameters of calculation stations, blade angles, blade-row efficiency and flow coefficient. The

calculation procedure based on the analysis by Flagg[11] is demonstrated in Figure 14. For a certain rotational speed, an initial first-vane total-to-static pressure ratio is specified. The flow velocities, flow angles, flow condition properties and mass flow rate at this pressure ratio level are then computed at station 1 and station 0 (for station definition, see Figure 12). Based upon the mass flow rate derived at station 1, flow conditions at the following calculation stations can be established with the help of angular momentum conservation, the continuity equation and the energy equation. Work done by a stage is calculated at station 2A using the Euler turbine equation. The rest of the stags follow the same procedure. After calculations go through all stages, major outputs are computed. If no choking occurs at any blade row, the initial pressure ratio is increased by an increment and the calculations are repeated with the new pressure ratio. If the choking point is located, the pressure ratio step will be enlarged and several repeats are run until stop for a certain corrected speed. The same procedure applies for other wheel rotational speeds.

When the calculations for all wheel speed levels are complete, off-design performance is then established in terms of equivalent mass flow rate vs. turbine expansion ratio and efficiency vs. turbine expansion ratio. Two corresponding maps can be generated. The equivalent mass flow rate and equivalent rotational speed which are used for off-design performance analysis are defined in Equation (24) and Equation (25) respectively.

$$\text{Equivalent mass flow rate} = \frac{W\sqrt{\theta}}{\delta} \qquad (24)$$

$$\text{Equivalent rotational speed} = N/\sqrt{\theta} \qquad (25)$$

Where W is the actual mass flow rate and N is rotational speed. δ is the reference pressure ratio, defined as the ratio of turbine inlet total pressure to the reference pressure. θ is the reference temperature ratio, defined as the ratio of absolute turbine inlet total temperature to the reference temperature. The reference pressure and temperature used in our case are the critical point, i.e., pressure 7.377 MPa and temperature 304.12K.

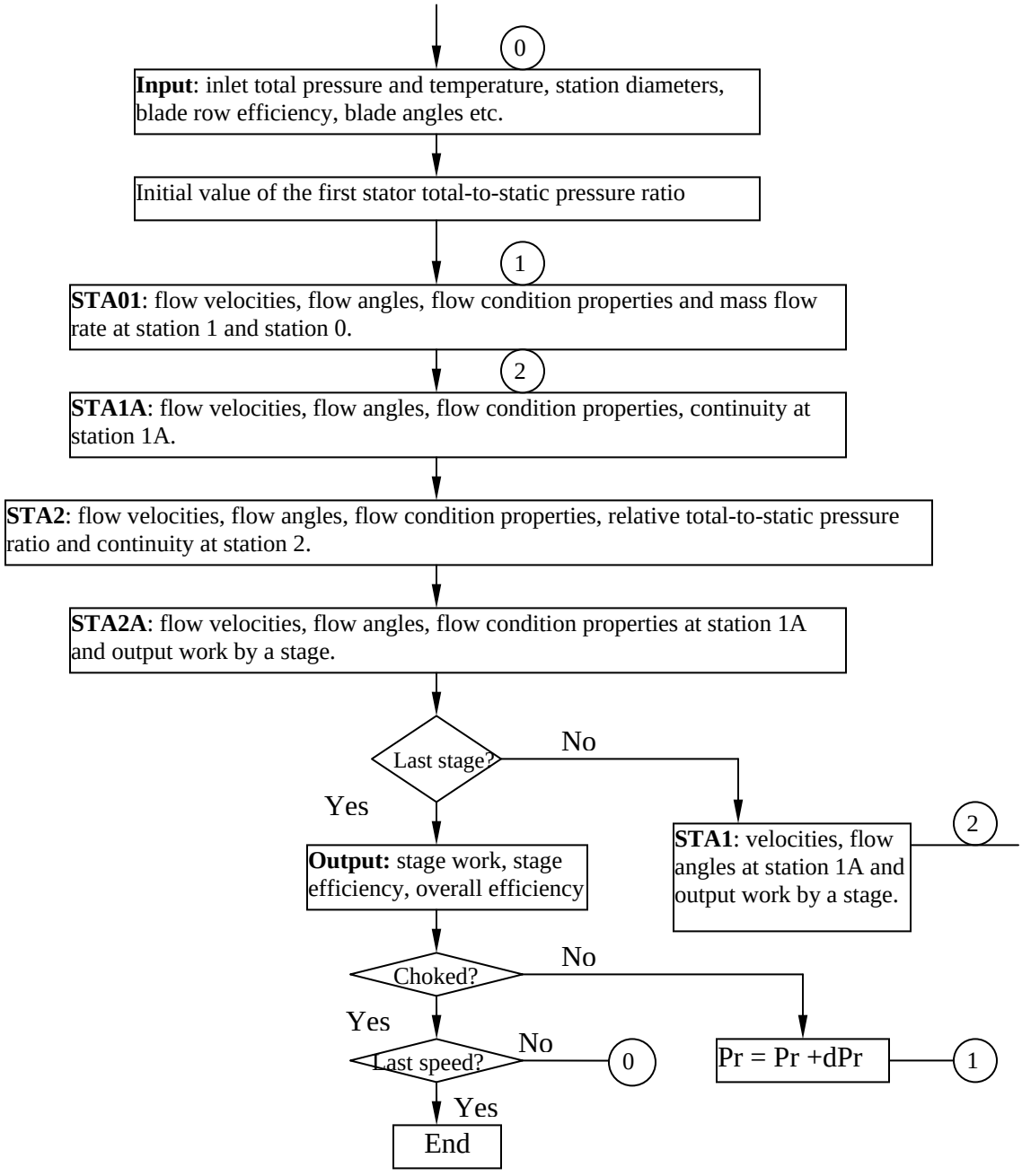

Figure 14. Calculation procedure of AXOD

AXOD Modifications (AXOD-MOD)

AXOD was also originally developed for ideal (semi-perfect) gas applications. In order to apply to our case, the code was modified by implementing real gas properties. The major modifications will be discussed in the following section.

In order to calculate the mass flow rate through sectors, local density should be calculated first. Since specific heat capacity Cp and the specific heat ratio γ are assumed to be constant across a blade row for an ideal gas, the static temperature can be readily computed by Equation (26) when the total-to-static pressure ratio is already known.

$$T_{s,1} = T_{t,0}\left[1 - \eta_s\left(1 - \delta_{ts}^{\frac{-(\gamma-1)}{\gamma}}\right)\right] \tag{26}$$

Where η_s is the stator efficiency, and δ_{ts} is the ratio of $P_{t,0}$ to $P_{s,1}$. The relation between $T_{s,1}$ and $T_{t,0}$ is more obvious in Figure 15.

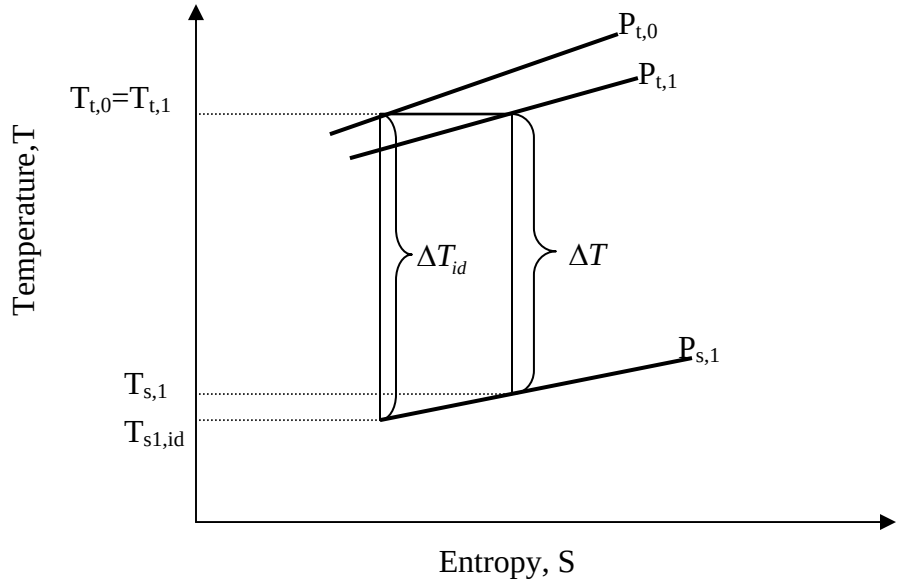

Figure 15. Definition of stator efficiency for ideal gas

Once the static pressure and the static temperature are already known, the local density is then obtained from the equation of state.

However, the total temperature (or the relative total temperature for the rotor) is not constant across the stator in the real gas case. Instead, the total enthalpy stays unchanged (see also Figure 13). According to the definition of the blade-row efficiency, the static enthalpy at the stator exit is determined by Equation (27):

$$H_{s,1} = H_{t,0} - \eta_s \left(H_{t,0} - H_{s1,id} \right) \tag{27}$$

Where $H_{t,0}$ is the stator inlet total enthalpy, $H_{s,1}$ is the stator exit static enthalpy, $H_{s1,id}$ is ideal static enthalpy at the stator exit so that the expansion process from the stator inlet total condition to exit static state condition is isentropic. The local temperature and density are obtained via the NIST property database when the static enthalpy and the static pressure are known.

The calculation of the static state condition based upon the total state condition has been discussed in the foregoing section and will not be repeated here.

When the expansion process occurs across a rotor, the relative total temperature and pressure at the rotor exit are adjusted by addition of an extra energy term due to the possible radial inflow or outflow.

$$\begin{cases} T_{tr,2} = T_{tr,1A} + \left(U_2^2 - U_{1A}^2 \right) / \left(2 \cdot Cp \right) \\ P_{tr,2} = P_{tr,1A} \left(\dfrac{T_{tr,2}}{T_{tr,1A}} \right)^{\gamma - 1 / \gamma} \end{cases} \tag{28}$$

Where subscript “tr” denotes the relative total condition.

For the real gas, the first relation in Equation (28) is replaced with

$$H_{tr,2} = H_{tr,1A} + \left(U_2^2 - U_{1A}^2\right)/2 \tag{29}$$

Because there is no loss associated with the radial flow shift, the relative total conditions at the rotor exit can then be established based on the inlet entropy and exit relative total enthalpy.

The process between the blade row exit and the following blade row inlet (for example, from station 1 to station 1A) is assumed to be adiabatic and isentropic. The flow conditions at a downstream calculation station can be attained by the relations:

$$\begin{cases} \Delta T_s = \left(V_1^2 - V_{1A}^2\right) \Big/ 2Cp \\ T_{s,1A} = T_{s,1} + \Delta T_s \\ P_{s,1A} = P_{s,1}\left(\dfrac{T_{s,1A}}{T_{s,1}}\right)^{\gamma-1/\gamma} \end{cases} \tag{30}$$

For the real gas, the energy equation is rewritten in a general form:

$$\Delta H_s = \left(V_1^2 - V_{1A}^2\right) \Big/ 2 \tag{31}$$

The static enthalpy at station 1A is then readily known by adding the enthalpy difference to the static enthalpy at station 1. With the isentropic assumption, the other static state conditions can be computed via interpolation in terms of entropy and the static enthalpy.

The actual work that is done by each stage is calculated using the Euler equation in terms of velocity diagrams. To complete the efficiency calculations, ideal (isentropic) work done by a stage has to be determined. When Cp and γ are constant, the ideal work

can be easily obtained using the relation (showing total efficiency calculation as an example):

$$\Delta H_{t,id} = CpT_{t,0}\left(1-\left(\frac{P_{t,2A}}{P_{t,0}}\right)^{\gamma-1/\gamma}\right) \tag{32}$$

When the real gas applies, ideal work is calculated in the following way: the total enthalpy and entropy are first obtained on the basis of inlet conditions. Since the inlet entropy is equal to the exit entropy, the ideal exit total enthalpy can then be determined based on pressure and entropy. The ideal work is then obtained by subtracting exit enthalpy from inlet total enthalpy.

One or more of three efficiencies may be referred to for different applications: total-to-total (total) efficiency is defined as the ratio of stage actual work to ideal work when the flow expands isentropically from the stage inlet total condition to the stage exit total state; total-to-static (static) efficiency is defined so that the stage exit velocity is considered to be a loss; rating efficiency is defined so that the swirl velocity at stage exit is accounted for as a loss. Figure 16 shows the relations between these three efficiencies which are expressed in Equations (33-35).

$$\eta_t = \frac{\Delta H_t}{\Delta H_{t,id}} \tag{33}$$

$$\eta_s = \frac{\Delta H_t}{\Delta H_{s,id}} \tag{34}$$

$$\eta_{at} = \frac{\Delta H_t}{\Delta H_{at,id}} \tag{35}$$

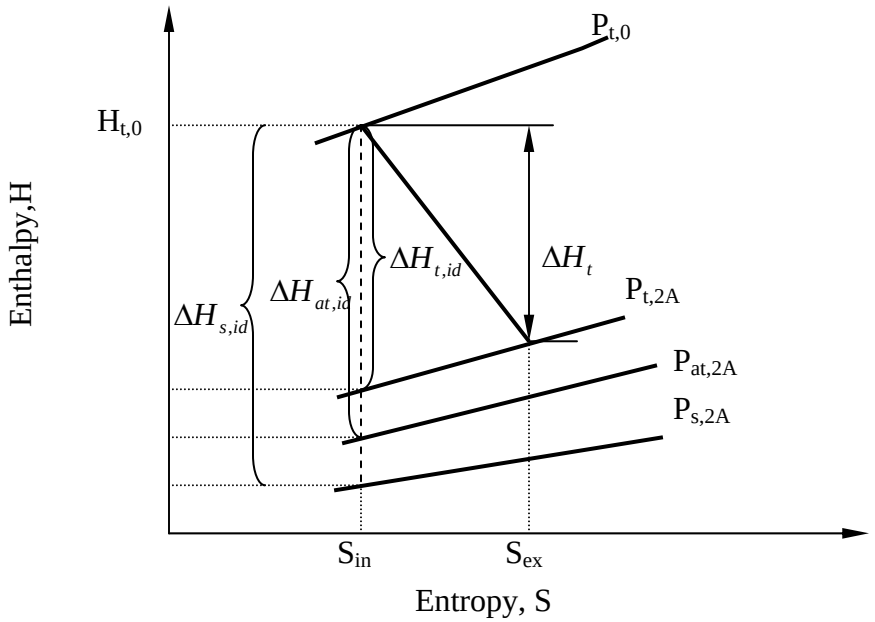

Figure 16. Definition of stage total efficiency, static efficiency and rating efficiency

Off-design Performance Maps

Although synchronization with the grid sets the mechanical speed of the turbine fixed, the turbine inlet stagnation temperature may decrease when the turbine runs at partial laod. The corrected speed, as defined in Equation (25), which is proportional to the square root of inlet stagnation temperature increases accordingly. The relations between efficiency, equivalent mass flow rate and pressure ratio at differnent corrected speeds are illustrated in Figure 17. The off-design performance maps can be used for cycle control analyis.

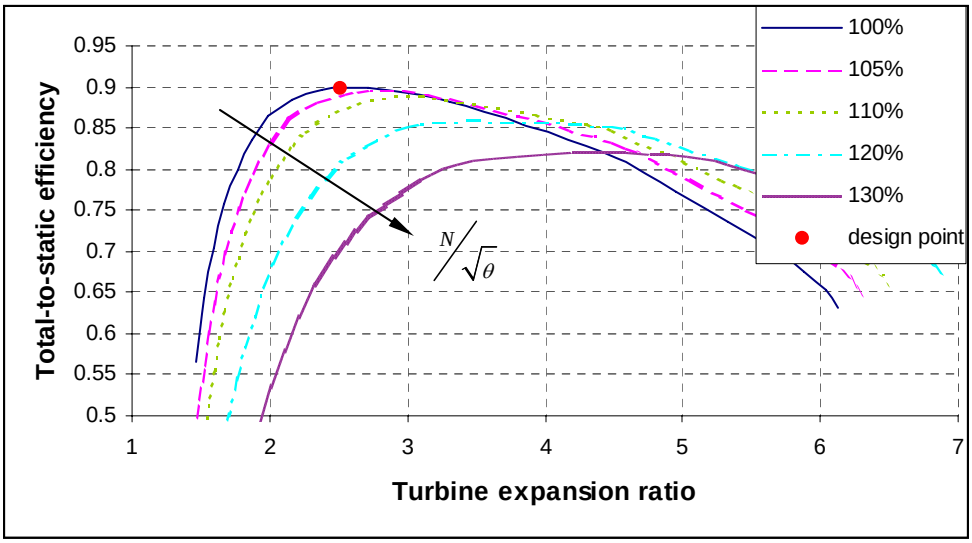

(a) Efficiency vs. turbine expansion ratio

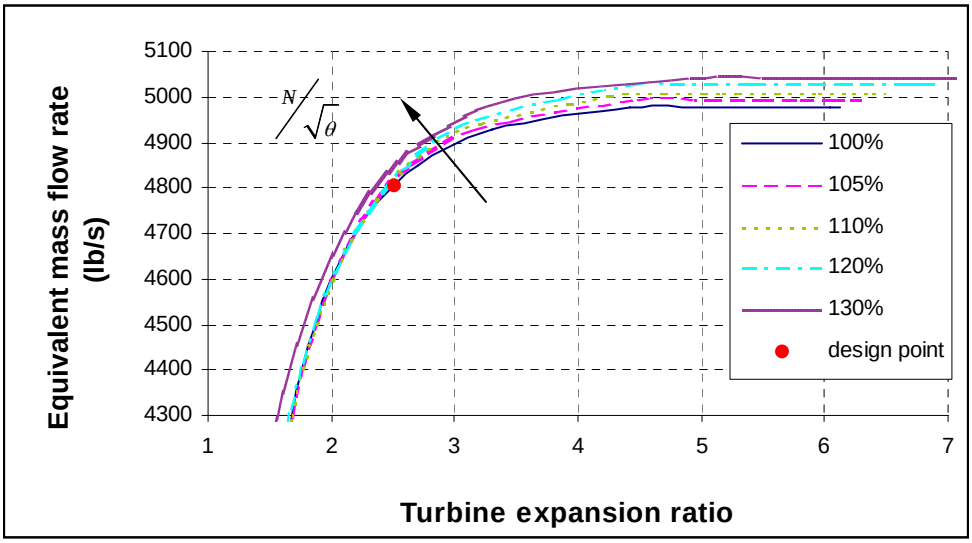

(b) Equivalent mass flow rate vs. turbine expansion ratio

Figure 17. Turbine off-design performance maps

Conclusions

Aerodynamic design of the turbine was completed for a supercritical CO_2 Brayton cycle under the assumption that mean blade diameters are kept constant through the turbine, and each stage assumes the same share of work and has the same velocity triangle. The analysis shows that dealing with CO_2 as a real gas is more appropriate since the ideal gas assumption results in overestimating power by 10.8%. With turbine inlet

temperature of 550^{o}C, inlet pressure of 19.4 MPa, power output of 450 MW and mass flow rate of 3644 kg/s, the design yields a compact and highly efficient S-CO_2 turbine with blade section length of 0.566 m, exit turbine diameter of 1.275 m and static efficiency of 0.897. The static efficiency value is 2% higher than the value of efficiency obtained by Dostal[1] using methods based upon steam turbine technology. Off-design performance maps are also established for the current turbine, which can be used for cycle control analysis.

Future work will focus on axial-flow compressor design at steady state, and on off-design performance map which will be used for cycle analysis. Cycle performance optimization will also be conducted to determine the features of the main compressor and the recompressing compressor. For turbine, optimum of degree of reaction will be established in this high-pressure turbomachine based upon the evaluation of a tradeoff between the effect of profile loss and the effect of leakage loss when leakage loss model becomes available. Stress analysis will be performed for both turbine and compressor under current design. A big challenge for seal design also awaits to be addressed in-depth due to presence of high-pressure differential across the turbine and compressor stage.

References

[1] Dostal V., M.J. Driscoll, P. Hejzlar, N.E. Todeas,"CO_2 Brayton Cycle Design and Optimization", MIT-ANP-TR-090, CANES, November 2002.

[2] Steward, W.L, " A Study of Axial Flow Turbine Efficiency Characteristics in Terms of Velocity Diagram Parameters". ASME Paper 61-WA-37, 1961.

[3] Glassman, A.J., " Computer Code for Preliminary Sizing Analysis of Axial-Flow Turbines". NASA CR-4430, 1992

[4] Glassman, A.J., "Blading Models for TURBAN and CSPAN Turbomachine Design Codes". NASA CR-191164, 1993.

[5] Zweifel, O., "The Spacing of Turbo-Machine Blading, Especially with Large Angular Deflection". Brown Boveri Rev., vol. 32, no. 12, Dec. 1945, pp. 436—444

[6] NIST Standard Reference Database 12, NIST Thermodynamics and Transport Properties of Pure Fluids—NIST pure Fluids, Version 5.0,2000

[7] Fielding, Leslie. Turbine design :the effect on axial flow turbine performance of parameter variation /by Leslie Fielding. New York : ASME Press, 2000.

[8] Cohen, H. et al., "Gas Turbine Theory", 3rd edition, 5th impression, Longman Scientific & Technical, Copublished in the United States with John Wiley & Sons, Inc., New York, 1991

[9] Muto Y., T. Nitawaki, Y. Kato, "Comparative Design Study of Carbon Dioxide Gas Turbine and Helium Gas Turbine for HTGR Power Plant". Proceedings of ICAPP'03. May 4—7,2003.

[10] Glassman, A.J., “Modeling Improvements and User Manual for Axial Flow Turbine Off-Design Performance”. NASA CR-195370, 1994.

[11] Flagg, E.E., “Analytical Procedure and Computer Program for Determining The Off-Design Performance of Axial Flow Turbines”. NASA CR-710, 1967.

Appendix A

4 STAGE-TURBAN INPUT VARIABLES

Inlet turbine temperature	TTIN = 550 ^{o}C
Inlet turbine pressure	PTIN = 19.4 MPa
Gas viscosity	MU = 2.352E-5 N-sec/m^2
Gas constant	R = 188.9 J/kg-K
Specific heat ratio	GAM = 1.235
Inlet blade mean diameter	DIN = 1.016 m
Exit blade mean diameter	DEX = 1.016 m
Rotational speed	RPM = 3600 rpm
Shaft power	POW = 450 MWt
Mass flow rate	W = 3644.3 kg/sec
Vane exit angle	ALPHA = 66
Minimum number of stages	NMIN = 4
Maximum number of stages	NMAX = 4
Vane exit angle indicator	IALPH = 0
Indicator of input diameter	IDIAM = 2
Indicator of velocity triangle	IVD = 6
Indicator of exit vanes	IEV = 0
Indicator of shaft power	IPR = 0
Indicator of units	IU = 2
Indicator of meanline shape	IMID = 0
Indicator of aspect ratio	IAR = 2
Stage reaction	REACT = 0.5
Turbine loss coefficient	KLOSS = 0.40
Squared ratio of stage-exit to stage-average velocities	E = 1.0